Journal of Neuroradiology (2015) 42, 212—221

Available online at ScienceDirect www.sciencedirect.com

Elsevier Masson France EM|consulte www.em-consulte.com/en

ORIGINAL ARTICLE

Addition of MR imaging features and genetic biomarkers strengthens glioblastoma survival prediction in TCGA patients

Manal Nicolasjilwan[a], Ying Hu[b], Chunhua Yan[b], Daoud Meerzaman[b], Chad A. Holder[c], David Gutman[d], Rajan Jain[e], Rivka Colen[f], Daniel L. Rubin[g], Pascal O. Zinn[h], Scott N. Hwang[i], Prashant Raghavan[a], Dima A. Hammoud[j], Lisa M. Scarpace[k], Tom Mikkelsen[k], James Chen[l], Olivier Gevaert[m], Kenneth Buetow[n], John Freymann[o], Justin Kirby[o], Adam E. Flanders[p], Max Wintermark[a,q,*], on behalf of the TCGA Glioma Phenotype Research Group

[a] *Division of Neuroradiology, University of Virginia Health System, Charlottesville, VA, United States*
[b] *Center for Biomedical Informatics & Information Technology, National Cancer Institute, Bethesda, MD, United States*
[c] *Department of Radiology and Imaging Sciences Division of Neuroradiology, Emory University School of Medicine, Atlanta, GA, United States*
[d] *Department of Biomedical Informatics, Emory University, Atlanta, GA, United States*
[e] *Departments of Radiology and Neurosurgery, Henry Ford, Detroit, MI, United States*
[f] *Division of Neuroradiology, The University of Texas MD Anderson Cancer Center, Houston, TX, United States*
[g] *Department of Radiology and Medicine (Biomedical Informatics Research), Stanford University, Stanford, CA, United States*
[h] *Department of Neurosurgery, The University of Texas MD Anderson Cancer Center, Houston, TX, United States*
[i] *Neuroradiology Section, St. Jude Children's Research Hospital, Memphis, TN, United States*

Abbreviations: ADC, average diffusion coefficient; AIC, Akaike's information criterion; AUC, area under the curve; GBM, glioblastoma; GSEA, gene set enrichment analysis; KPS, Karnofsky Performance Score; NCI, National Cancer Institute; NHGRI, National Human Genome Research Institute; TCGA, The Cancer Genome Atlas; TCIA, The Cancer Imaging Archive (http://cancerimagingarchive.net); VASARI, Visually AcesSAble Rembrandt Images (https://wiki.cancerimagingarchive.net/display/Public/VASARI+Research+Project); WHO, World Health Organization.

* Corresponding author. Department of Radiology and Medical Imaging, Division of Neuroradiology, PO Box 800170, 22908-0170 Charlottesville, VA, United States. Tel.: +1 434 982 1736; fax: +1 434 982 5753.
E-mail address: max.wintermark@gmail.com (M. Wintermark).

http://dx.doi.org/10.1016/j.neurad.2014.02.006

[j] *Radiology and Imaging Sciences, National Institutes of Health, Clinical Center, Bethesda, MD, United States*
[k] *Departments of Neurosurgery, Henry Ford, Detroit, MI, United States*
[l] *Division of Neuroradiology, University of California, San Diego, CA, United States*
[m] *Center for Cancer Systems Biology (CCSB) & Department of Radiology, Stanford University, Stanford, CA, United States*
[n] *Arizona State University Life Science, Tempe, AZ, United States*
[o] *SAIC-Frederick, Inc., Frederick, MD, United States*
[p] *Division of Neuroradiology, Thomas Jefferson University Hospital, Philadelphia, PA, United States*
[q] *CHU de Vaudois, Department of Radiology, Lausanne, Switzerland*

Available online 2 July 2014

KEYWORDS
Glioblastoma;
Magnetic resonance imaging;
Genetics;
Survival;
Prognosis

Summary
Purpose: The purpose of our study was to assess whether a model combining clinical factors, MR imaging features, and genomics would better predict overall survival of patients with glioblastoma (GBM) than either individual data type.
Methods: The study was conducted leveraging The Cancer Genome Atlas (TCGA) effort supported by the National Institutes of Health. Six neuroradiologists reviewed MRI images from The Cancer Imaging Archive (http://cancerimagingarchive.net) of 102 GBM patients using the VASARI scoring system. The patients' clinical and genetic data were obtained from the TCGA website (http://www.cancergenome.nih.gov/). Patient outcome was measured in terms of overall survival time. The association between different categories of biomarkers and survival was evaluated using Cox analysis.
Results: The features that were significantly associated with survival were: (1) clinical factors: chemotherapy; (2) imaging: proportion of tumor contrast enhancement on MRI; and (3) genomics: *HRAS* copy number variation. The combination of these three biomarkers resulted in an incremental increase in the strength of prediction of survival, with the model that included clinical, imaging, and genetic variables having the highest predictive accuracy (area under the curve 0.679 ± 0.068, Akaike's information criterion 566.7, $P < 0.001$).
Conclusion: A combination of clinical factors, imaging features, and *HRAS* copy number variation best predicts survival of patients with GBM.

Introduction

Recent research in glioblastoma (GBM) treatment has focused on identification of biomarkers that may predict patient outcome, and may consequently impact therapeutic decisions through selection of more aggressive therapies for tumors with worse prognosis. The impact of clinical factors on patient outcome [1—4] and the correlation between MR imaging features of GBM and survival [5—11] have been previously studied. Similarly, the association between genomic biomarkers and patient outcome has received growing attention, in particular with the recent introduction of anti-angiogenetic drugs [12—16]. Only few studies so far have attempted to integrate clinical factors, imaging biomarkers (usually not evaluated across observers in a standardized fashion), and tumor gene expression data into a statistical model that would potentially provide a robust predictor of patient outcome than each individual type of data [17]. The purpose of our study was to assess whether such a model combining clinical factors, MR imaging features (assessed using standardized semantic imaging features across multiple observers), and genomics would predict patient survival more reliably than any individual data type.

Materials and methods

Study data

Our study was conducted leveraging the TCGA project (http://www.cancergenome.nih.gov/) of the National Cancer Institute (NCI) and National Human Genome Research Institute (NHGRI), which aims to catalogue gene mutations associated with cancer. One hundred and two patients with pathology proven GBM were included in this study. Their MR imaging studies were made available through The Cancer Imaging Archive (http://www.cancerimagingarchive.net). Clinical data were obtained from the Open Access Data Tier of the TCGA website, and Health Insurance Portability and Accountability Act of 1996 (HIPAA) de-identified clinical data.

Gene expression, mutation and copy number data were obtained from the TCGA data portal (https://tcga-data.nci.nih.gov). Three sets of genetic metadata were separately considered for the current study:

- genes with *P*-value < 0.05 in univariate COX model analysis of gene expression and overall survival were assessed further with gene set enrichment analysis (GSEA). GSEA is

a method to evaluate the expression of genes in the context of pathways. A significant pathway means that gene expression in these pathways is significantly different compared to a random gene set. We used a hypergeometric test to detect significant biological pathways;
- the mutation status of specific genes of interest identified in previous work (*EGFR*, *ERBB2*, *IDH1*, *NF1*, *PDGFRA*, *PIK3CA*, *PIK3R1*, *PTEN*, *RB1* and *TP53*) was also evaluated [18];
- as part of a copy number analysis, raw data were first converted into an ordinal ranking (homozygous deletion, heterozygous deletion, wild type, low level amplification, high level amplification), as described by the Computational Biology Center at Memorial Sloan-Kettering Cancer Center (http://www.cbioportal.org/public-portal/) prior to Cox survival analysis.

Imaging review

Six neuroradiologists from the University of Virginia Health System, Thomas Jefferson University Hospital, Emory University, MD Anderson Cancer Center and the National Institute of Health, independently reviewed the MR images of 102 patients, using Clear Canvas workstations, which allow visualization as well as annotation and markup of DICOM images (customized version of Clear Canvas to support the capture of markups in Annotation and Image Markup [AIM] format, available at https://wiki.nci.nih.gov/x/z4X3Ag). The VASARI feature scoring system for human gliomas (https://wiki.cancerimagingarchive.net/display/Public/VASARI+Research+Project) was employed for the interpretation of the MR images to ensure interobserver consistency. The VASARI scoring system (Table 1) includes 30 semantic descriptors of imaging features of brain tumors clustered by categories pertaining to lesion location, morphology of the lesion substance, morphology of the lesion margin, alterations in the vicinity of the lesion, and extent of tumor resection [7,19]. For each feature, the scoring system incorporates discrete qualitative, semi-quantitative, or quantitative values, appropriate to the nature of the feature assessed.

Statistical analysis

The 102 study patients were split into a training set of 68 patients and a separate testing set of 34 patients using a stratified sampling method. Stratified sampling was selected because of the small sample size and the skewed survival distribution, and because it ensures an approximately equal survival distribution of subjects between the training and testing data. The split data are also more representative of the population than the random sampling. Samples were sorted by survival in an ascending order. For every three samples, the first two samples were chosen as the training dataset and the third sample was selected as the testing dataset. Models were created in the training dataset and validated in the testing dataset.

Associations between survival (outcome) and different individual categories of predictors including clinical variables (Table 2), imaging features (Table 1), tumor gene expression, mutation, and copy number variation (Table 3) were assessed using univariate Cox regression models. Clinical, genetic, and imaging data were checked for co-linearity. Non-collinear, predicting variables shown as significant in the univariate Cox regression models were retained and included in several multivariate Cox regression models incorporating the clinical, imaging and/or genomic datasets using stepwise covariate model-building strategies. The models were compared with Akaike's Information Criterion (AIC) to evaluate the model fitness, with the baseline model with clinical data only used as reference for comparisons [20]. A lower AIC value indicates a better model. AUC (area under curve) analysis was also used to measure the accuracy of prediction. A higher AUC value indicates that the model is better at predicting survival. The model using only clinical data was used as the reference. Statistical models were corrected for multiple comparisons using false discovery rate (FDR) procedure.

Results

Study population demographics

The clinical and imaging characteristics of our 102 patients are reported in Tables 2 and 1, respectively. We calculated the association of 17,787 genes with expression data, 10 genes with mutation data and 14 genes with copy number data. The median survival was 324.0 days (25 percentile: 144.5, 75 percentile: 578.8, minimum: 6.0, maximum: 1757.0).

Correlation between clinical variables and survival

Univariate Cox model analyses demonstrated that three clinical variables were significantly correlated to survival with an unadjusted P-value < 0.05 (Table 2). These included radiation therapy ($P < 0.001$), chemotherapy ($P < 0.001$), and age at initial diagnosis ($P = 0.021$). The 6 patients who did not receive radiation therapy had a median survival of 66 days compared to median survival of 389 days in the 96 patients with radiation therapy. The 14 patients who did not receive chemotherapy had a median survival of 132 days compared to the median survival of 454 days in the 88 patients with chemotherapy. An increased age at the initial pathological diagnosis was associated with a shorter survival ($P = 0.021$). All clinical features were used to build survival models in a stepwise fashion. Only chemotherapy was significant in the multiple clinical feature model.

Correlation between VASARI imaging features and survival

Univariate Cox model analyses showed that four VASARI features were associated with a shorter survival time with an unadjusted P-value < 0.05: higher proportion of enhancing tumor ($P = 0.009$), a higher T1/FLAIR ratio ($P = 0.022$), and tumor location ($P = 0.029$) and side ($P = 0.049$) (Table 1). The T1/FLAIR ratio measures the ratio between the size of the portion of the tumor that is hypointense on T1-weighted images in relation to the extent of FLAIR signal abnormality corresponding to the tumor. A higher T1/FLAIR ratio

Table 1 Correlation between Vasari imaging features and survival time on univariate Cox analysis.

Vasari imaging features			Values in our study population (counts)	Coefficient	Hazard ratio	Standard error	*P*-value
F1	Tumor location	1 = frontal	32/102	−0.609	0.544	0.278	0.029
		2 = temporal	45/102				
		3 = insular	3/102				
		4 = parietal	13/102				
		5 = occipital	9/102				
F2	Side of tumor epicenter	1 = right	52/102	−0.525	0.592	0.267	0.049
		2 = center/bilateral	0/102				
		3 = left	50/102				
F3	Eloquent brain involved	1 = none	60/102	−0.479	0.620	0.352	0.174
		2 = speech motor	7/102				
		3 = speech receptive	14/102				
		4 = motor	12/102				
		5 = vision	9/102				
F4	Enhancement quality	1 = none	0/102	0.5961	1.815153	0.596921	0.31792
		2 = mild/minimal	6/102				
		3 = marked/avid	96/102				
F5	**Proportion enhancing**	**1 = not available**	**0/102**	**−0.637**	**1.891**	**0.243**	**0.009**
		2 = none (0%)	**0/102**				
		3 = < 5%	**9/102**				
		4 = 6—33%	**71/102**				
		5 = 34—67%	**21/102**				
		6 = 68—95%	**5/102**				
		7 = > 95%	**0/102**				
		8 = all (100%)	**0/102**				
F6	Proportion non-enhancing	1 = not available	0/102	−0.155	0.857	0.173	0.372
		2 = none (0%)	18/102				
		3 = < 5%	33/102				
		4 = 6—33%	29/102				
		5 = 34—67%	12/102				
		6 = 68—95%	10/102				
		7 = > 95%	0/102				
		8 = all (100%)	0/102				
F7	Proportion necrosis	1 = not available	0/102	0.171	1.187	0.254	0.500
		2 = none (0%)	3/102				
		3 = < 5%	18/102				
		4 = 6—33%	41/102				
		5 = 34—67%	30/102				
		6 = 68—95%	10/102				
		7 = > 95%	0/102				
		8 = all (100%)	0/102				
F8	Cysts	1 = no	97/102	−0.490	0.613	0.721	0.497
		2 = yes	5/102				

Table 1 (*Continued*)

Vasari imaging features			Values in our study population (counts)	Coefficient	Hazard ratio	Standard error	*P*-value
F9	Multifocal or multicentric	1 = not available	0/102	−0.546	0.579	0.443	0.218
		2 = focal	94/102				
		3 = multifocal	5/102				
		4 = multicentric	1/102				
		5 = gliomatosis	2/102				
F10	T1/FLAIR ratio	1 = expansive (T1∼FLAIR)	64/102	−0.529	1.697	0.230	0.022
		2 = mixed (T1 < FLAIR)	8/102				
		3 = infiltrative (T1 < FLAIR)	30/102				
F11	Thickness of enhancing margin	1 = not available	0/102	0.596	1.815	0.597	0.318
		2 = none	0/102				
		3 = thin	7/102				
		4 = thick/solid	95/102				
F13	Definition of the non-enhancing margin	1 = not available	0/102	−0.179	0.836	0.435	0.681
		2 = smooth	13/102				
		3 = irregular	92/102				
F14	Proportion of edema	1 = not available	0/102	−0.236	0.790	0.206	0.251
		2 = none (0%)	1/102				
		3 = < 5%	19/102				
		4 = 6—33%	32/102				
		5 = 34—67%	48/102				
		6 = 68—95%	2/102				
		7 = > 95%	0/102				
		8 = All (100%)	0/102				
F16	Hemorrhage	1 = no	68/102	0.045	1.046	0.279	0.872
		2 = yes	34/102				
F17	Diffusion	1 = no image	0/102	−0.273	0.761	0.405	0.500
		2 = facilitated	49/102				
		3 = restricted	11/102				
		4 = neither/equivocal/both	42/102				
F18	Pial invasion	1 = no 2 = yes	60/102 42/102	−0.179	0.836	0.274	0.512
F19	Ependymal invasion	1 = no 2 = yes	41/102 61/102	0.263	1.301	0.270	0.329
F20	Cortical involvement	1 = no 2 = yes	10/102 92/102	−0.569	0.566	0.367	0.122
F21	Deep white-matter invasion	1 = no 2 = yes	42/102 60/102	−0.527	0.590	0.274	0.054

Table 1 (*Continued*)

Vasari imaging features			Values in our study population (counts)	Coefficient	Hazard ratio	Standard error	*P*-value
F22	Non-enhancing tumor crosses midline	1 = not available	0/102	0.318	1.374	0.331	0.337
		2 = no	80/102				
		3 = yes	22/102				
F23	Enhancing tumor crosses midline	1 = not available	0/102	1.007	2.738	0.529	0.057
		2 = no	92/102				
		3 = yes	10/102				
F24	Satellites	1 = no 2 = yes	77/102 25/102	0.130	1.139	0.327	0.691
F25	Calvarial remodeling	1 = no 2 = yes	100/102 2/102	−0.139	0.871	0.724	0.848
F29 & F30	Lesion size	Major axis length	76.80598 (20.60491)	0.007	1.007	0.007	0.283
		Minor axis length	49.89373 (12.32175)	−0.001	0.999	0.012	0.934
			Mean(SD)				

In univariate Cox model analyses, four VASARI features were associated with shorter survival time with an unadjusted *P*-value < 0.05: higher proportion of enhancing tumor ($P = 0.009$), higher T1/FLAIR ratio ($P = 0.022$), and tumor location ($P = 0.029$) and side ($P = 0.049$). Only the proportion of tumor enhancing (bolded) was significant in the multiple clinical feature model.

indicates a more infiltrative tumor. Tumor location in the frontal lobe ($P = 0.029$) and tumors on the right side ($P = 0.049$) correlated with a longer survival. Only the proportion of enhancing tumor was significant in the multiple clinical feature model (Fig. 1).

Correlation between genomics and survival

Cox model analyses revealed that three genes with copy number variations, *PIK3R1* ($P = 0.005$), *AKT1* ($P = 0.024$), and *HRAS* ($P = 0.071$), and two genes with mutation, *PDGFRA* ($P = 0.028$) and *NF1* ($P = 0.082$) were associated with survival (Table 3). However, none of these genes had FDR (false discovery rate) adjusted *P*-value < 0.050 [21].

We used a Cox model analysis to investigate association between survival and tumor gene expression. A total of 724 genes were associated with survival with an adjusted *P*-value < 0.05 in the training dataset; however, none of the genes associated with survival passed the FDR test. Therefore, we carried out a gene set enrichment analysis (GSEA) of the 724 genes in order to select genes in significant biological pathways. This analysis revealed three gene categories

Table 2 Correlation between clinical features and survival time on univariate Cox analysis.

Clinical variables	Values in our study population (mean ± standard deviation or counts)	Coefficient	Hazard ratio	Standard error	*P*-value
Age at initial pathological diagnosis [years]	57.7 ± 14.6	0.023	1.023	0.010	0.021
Gender	66 males, 36 females	0.275	1.317	0.276	0.318
Ethnicity	8 Hispanic or Latino; 94 non-Hispanic or Latino	1.302	3.676	1.033	0.208
Race	83 Caucasian, 6 African-Americans, 5 Asians	0.446	1.562	0.391	0.255
Radiation therapy	96 yes, 6 no	−3.298	0.037	0.634	< 0.001
Chemotherapy	**88 yes, 14 no**	**−1.311**	**0.270**	**0.339**	**< 0.001**
Hormonotherapy	1 yes, 101 no	−0.049	0.952	1.014	0.962
Immunotherapy	2 yes, 100 no	−0.019	1.019	0.724	0.979

In univariate Cox model analyses, three clinical variables were correlated with survival with an unadjusted *P*-value < 0.05. These included radiation therapy ($P < 0.001$), chemotherapy ($P < 0.001$), and age at initial diagnosis ($P = 0.021$). Only chemotherapy (bolded) was significant in the multiple clinical feature model.

Table 3 Correlation between tumor gene expression and survival on Cox analysis.

Type of genetic analysis	Genes	Coefficient	Hazard ratio	Standard error	*P*-value
Copy number	*PIK3R1*	1.588	4.896	0.566	0.005
	AKT1	2.602	13.492	1.155	0.024
	HRAS	**1.125**	**3.080**	**0.623**	**0.071**
Mutation	*PDGFRA*	2.463	11.741	1.118	0.028
	NF1	−0.713	0.490	0.480	0.082
Gene set enrichment analysis (GSEA)	*FSHB*	1.311	3.709	0.636	0.039
	FSHR	0.812	2.253	0.446	0.069
	LHCGR	1.022	2.779	0.431	0.017
	TSHB	0.787	2.198	0.460	0.087
	TSHR	−0.370	0.689	0.282	0.188
	PRSS2 (neuroactive ligand-receptor interaction pathway)	0.463	1.589	0.255	0.069
	LDHAL6A	−0.854	0.425	0.642	0.183
	LDHAL6B	−1.303	0.271	0.601	0.030
	LDHA (cysteine metabolism pathway)	0.356	0.356	0.163	0.029
	EFNA5	−0.723	0.485	0.390	0.063
	EPHA5 (Ephrin A reverse signaling pathway)	0.190	1.210	0.130	0.144

Cox model analyses revealed that three genes with copy number variations, *PIK3R1* ($P = 0.005$), *AKT1* ($P = 0.024$), and *HRAS* ($P = 0.071$), and two genes with mutation, *PDGFRA* ($P = 0.028$) and *NF1* ($P = 0.082$) were associated with survival. The gene set enrichment analysis (GSEA) revealed three gene categories associated with survival with an unadjusted *P*-value < 0.050. These included: (1) *FSHB*, *FSHR*, *LHCGR*, *TSHB*, *TSHR*, *PRSS2* genes in Neuroactive ligand-receptor interaction ($P = 0.012$); (2) *LDHAL6A*, *LDHAL6B*, *LDHA* genes in Cysteine metabolism ($P = 0.030$); and (3) *EFNA5* and *EPHA5* genes in Ephrin A reverse signaling ($P = 0.009$). Only *HRAS* (bolded) copy number variation was significant in the multiple clinical feature model.

associated with survival with an unadjusted *P*-value < 0.050. These included:

- *FSHB*, *FSHR*, *LHCGR*, *TSHB*, *TSHR*, *PRSS2* genes in Neuroactive ligand-receptor interaction;
- *LDHAL6A*, *LDHAL6B*, *LDHA* genes in Cysteine metabolism;
- *EFNA5* and *EPHA5* genes in Ephrin A reverse signaling.

Only *HRAS* copy number variation was significantly associated with survival in the multiple genetic feature model.

Multivariate Cox analysis of the association between combined biomarkers and survival

Stepwise multivariate Cox's models were used to assess the association between overall survival time and the clinical data, VASARI imaging features and genomic variations shown as statistically significant in the above-mentioned Cox analyses (Table 4). Models were evaluated with AIC values for the model fitness and AUC values for the model prediction power. The clinical variable ''chemotherapy'', the imaging variable ''portion of the tumor enhancing'' and *HRAS* copy number variation are the only variables that remained significant in the multivariate analysis. The AIC value for the clinical data only model was 744.0 and the one for the clinical and imaging data was 739.8. The AIC value for the clinical and genomic data model was smaller, 569.9, indicating a better model. The AIC value for the clinical, imaging and genomic data was the smallest, 566.7, indicating the best model. AUC analysis led to the same conclusion, supporting the concept that the model including clinical, imaging and genomic data is the best predictor for survival. As designed, we use the testing data to validate the model, AUC analysis led to the same conclusion with the combined model with AUC = 0.679 ± 0.068 comparing to AUC values for chemotherapy = 0.575 ± 0.029, chemotherapy and proportion enhancing = 0.589 ± 0.030, chemotherapy and *HRAS* = 0.560 ± 0.063. That supports the notion that the model including clinical, imaging and genomic data is the best predictor for survival.

Discussion

Accurate classification of gliomas is important as the treatment modalities are substantially different between WHO grade III and IV tumors. Patients with GBM have the worst prognosis with a median survival of approximately 12 months despite advances in surgery, radiation therapy, and chemotherapy [22—24]. The current histopathology-based classification system for gliomas is complicated by considerable interobserver variability [25]. Moreover, the existence of different subclasses with varying response to treatment within similar histologic grades of glioma has been shown [25—27]. Therefore, a classification using more reliable biomarkers has been postulated as a critical element to improve treatment selection and outcome.

The association of clinical variables with the outcome of GBM patients has been extensively studied in the

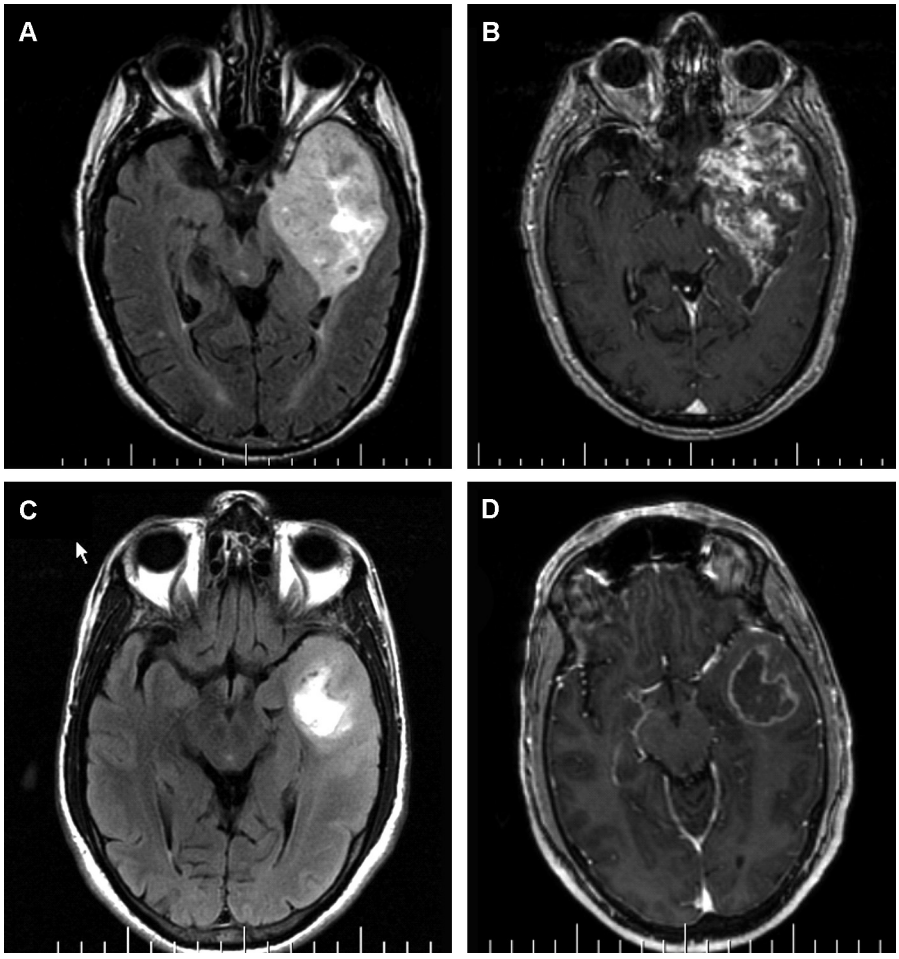

Figure 1 A and C. FLAIR and (B and D) post-contrast T1-weighted images in two patients with left temporal GBM. A and B. In patient #1, enhancement involves nearly the entirety of the tumor. Patient #1 survived 82 days after the MRI scan. C and D. In patient #2, enhancement involves only a small fraction of the tumor, basically a rim around the central necrosis. Patient #1 survived 467 days after the MRI scan.

literature. Among established independent predictors of poor outcome are older age (greater than 60 years), lower Karnofsky Performance Score (KPS), and incomplete tumor resection [1,3,4]. Barker et al. [4] also found in a population of 301 GBM patients that a more extensive surgical resection was associated with a better response to radiation therapy. Our univariate analysis demonstrated that three clinical features are associated with survival with a *P*-value < 0.05, including radiation therapy, chemotherapy, and age at initial diagnosis. Multivariate analysis only retained chemotherapy as significantly associated with improved survival.

Table 4 Multivariate analysis of the correlation between combined biomarkers and survival adjusted by age, race, and gender.

Model	Variables included in model	df	AIC	AUC mean ± standard deviation	*P*-value
Clinical data	Chemotherapy	3	744.0	0.575 ± 0.029	Not applicable
Clinical data and genomics	Chemotherapy, *HRAS*	4	569.9	0.560 ± 0.063	< 0.001
Clinical and imaging data	Chemotherapy, proportion enhancing	4	739.8	0.589 ± 0.030	0.012
Clinical and imaging data and genomics	Chemotherapy, proportion enhancing and *HRAS*	5	566.7	0.679 ± 0.068	< 0.001

The model with smaller AIC is a better fit model. The model with larger AUC has better prediction power. Df indicated the variables used in the model-building. *P*-values (< 0.05) showed that there is a significant difference when comparing the combined models to the baseline clinical model. The model that best predicted survival (highest AUC, smallest AIC) included clinical and imaging data and genomics.

Several studies have evaluated the prognostic value of the imaging features of GBM. In a recent study of 393 GBM patients by Chaichana et al. [5], periventricular location of the tumor was associated with worse survival. A retrospective study by Murakami et al. [6] of 79 GBM patients demonstrated that lower ADC values within the tumor correlated with shorter survival. A study by Pope et al. [7] of 15 imaging features of high-grade gliomas, including 41 grade III gliomas and 110 GBMs, demonstrated that the absence of enhancing tumor, the absence of edema and the absence of satellite or multifocal lesions correlated with a doubling of the median survival. In a series of 141 grade III and IV gliomas, Steltzer et al. [9] showed that involvement of the corpus callosum is a poor prognostic sign. In our study, we assessed the prognostic value of a systematic scoring system for the MR imaging features of GBM. Features that were associated with poor outcome on the basis of univariate analyses included the proportion of tumor enhancing, and a higher T1/FLAIR ratio of the tumoral signal abnormality, which corresponds to a more infiltrative tumor. These results are consistent as they include features that likely denote more aggressive tumor behavior. The association of tumoral involvement of the visual cortex with a worse prognosis possibly relates to the fact that this location precludes complete surgical resection. Location of the tumor in the frontal lobe and in the right cerebral hemisphere correlated with longer survival. This may reflect that frontal lobe resection and right hemispheric lesion resection in particular can usually be more extensive than for other locations, as the majority of patients are left hemisphere dominant. The multivariate analysis showed that only the proportion of tumor enhancing significantly correlated with a worse survival. This is concordant with a well-established imaging criterion that associates enhancement with more aggressive tumor behavior [7,17]. Likewise, surgical biopsies and resections primarily target the enhancing portion of the tumor with the intent to sample and/or resect the higher grade component [28].

A number of genes among hundreds of currently identified tumor expression genes have been shown to have a predictive value in terms of GBM patient survival [10,13]. The Cancer Genome Atlas Network recently cataloged recurrent genomic abnormalities in GBM, which allowed a robust gene expression-based molecular classification of GBM into 4 subtypes: proneural, neural, classical, and mesenchymal [12]. Response to aggressive therapy appears to differ by subtype, with the greatest benefit in the classical subtype and no benefit in the proneural subtype. Our multivariate genomic analysis demonstrated that only *HRAS* copy number variation correlated with poorer survival. The *HRAS* gene is located on the short (p) arm of chromosome 11. It encodes for a GTPase enzyme also referred to as transforming protein p21, which is involved in regulating cell division in response to growth factor stimulation. *HRAS* is a proto-oncogene, and *HRAS* mutations are encountered in bladder, kidney and thyroid cancers (http://ghr.nlm.nih.gov/gene/HRAS). Our finding of *HRAS* being prognostic of outcome in GBM patients is concordant with several prior reports that demonstrated the causative role of *HRAS* mutation in the induction of GBM [29] and its association with shorter survival [13]. This gene is not among those used by Verhaak et al. in the tumor gene expression-based classification of GBM [12] and likely plays a role in the genesis of GBM across all subtypes.

The incremental addition of clinical (chemotherapy), imaging (proportion of tumor enhancing) and genomic (*HRAS*) biomarkers resulted in an incremental increase in the strength of their association with survival. The best model was the one that included all three types of biomarkers. These results are promising as they suggest that the combination of imaging and genomic variables with conventional clinical variables adds significant value in terms of prognosticating outcome.

We acknowledge several limitations to our study. The most significant one is the lack of complete clinical information if our study patients. For instance, Karnofsky Performance Score, percentage of resection, details of the chemotherapy, etc. were not available and could not be incorporated in the statistical analysis.

In conclusion, our study demonstrates that a subset of clinical variables, VASARI imaging features, and tumor gene expression, considered in combination with each other, correlate significantly with GBM patients' survival. These results need to be confirmed in a larger database including more complete clinical information.

Disclosure of interest

The authors declare that they have no conflicts of interest concerning this article.

References

[1] Verger E, Valduvieco I, Caral L, et al. Does gender matter in glioblastoma? Clin Transl Oncol 2011;13:737—41.
[2] Marina O, Suh JH, Reddy CA, et al. Treatment outcomes for patients with glioblastoma multiforme and a low Karnofsky Performance Scale score on presentation to a tertiary care institution. Clinical article. J Neurosurg 2011;115:220—9.
[3] Allahdini F, Amirjamshidi A, Reza-Zarei M, et al. Evaluating the prognostic factors effective on the outcome of patients with glioblastoma multiformis: does maximal resection of the tumor lengthen the median survival? World Neurosurg 2010;73:128—34 [discussion e16].
[4] Barker 2nd FG, Chang SM, Larson DA, et al. Age and radiation response in glioblastoma multiforme. Neurosurgery 2001;49:1288—97 [discussion 1297—8].
[5] Chaichana K, Parker S, Olivi A, et al. A proposed classification system that projects outcomes based on preoperative variables for adult patients with glioblastoma multiforme. J Neurosurg 2010;112:997—1004.
[6] Murakami R, Sugahara T, Nakamura H, et al. Malignant supratentorial astrocytoma treated with postoperative radiation therapy: prognostic value of pretreatment quantitative diffusion-weighted MR imaging. Radiology 2007;243:493—9.
[7] Pope WB, Sayre J, Perlina A, et al. MR imaging correlates of survival in patients with high-grade gliomas. AJNR Am J Neuroradiol 2005;26:2466—74.
[8] Li X, Jin H, Lu Y, et al. Identification of MRI and 1H MRSI parameters that may predict survival for patients with malignant gliomas. NMR Biomed 2004;17:10—20.
[9] Steltzer KJ, Sauve KI, Spence AM, et al. Corpus callosum involvement as a prognostic factor for patients with high-grade astrocytoma. Int J Radiat Oncol Biol Phys 1997;38:27—30.

[10] Gutman DA, Cooper LA, Hwang SN, et al. MR imaging predictors of molecular profile and survival: multi-institutional study of the TCGA glioblastoma data set. Radiology 2013;267:560—9.
[11] Zolal A, Hejcl A, Malucelli A, et al. Distant white-matter diffusion changes caused by tumor growth. J Neuroradiol 2013;40:71—80.
[12] Verhaak RG, Hoadley KA, Purdom E, et al. Integrated genomic analysis identifies clinically relevant subtypes of glioblastoma characterized by abnormalities in PDGFRA, IDH1, EGFR, and NF1. Cancer Cell 2010;17:98—110.
[13] Serao NV, Delfino KR, Southey BR, et al. Cell cycle and aging, morphogenesis, and response to stimuli genes are individualized biomarkers of glioblastoma progression and survival. BMC Med Genomics 2011;4:49.
[14] Jung CS, Unterberg AW, Hartmann C. Diagnostic markers for glioblastoma. Histol Histopathol 2011;26:1327—41.
[15] Parsa AT. Functional validation confirms genomic phenotypes of glioblastoma with implications for targeted therapy. World Neurosurg 2011;75:573—4.
[16] Brennan C. Genomic profiles of glioma. Curr Neurol Neurosci Rep 2011;11:291—7.
[17] Zinn PO, Sathyan P, Mahajan B, et al. A novel volume-age-KPS (VAK) glioblastoma classification identifies a prognostic cognate microRNA-gene signature. PLoS One 2012;7:e41522.
[18] Phillips HS, Kharbanda S, Chen R, et al. Molecular subclasses of high-grade glioma predict prognosis, delineate a pattern of disease progression, and resemble stages in neurogenesis. Cancer Cell 2006;9:157—73.
[19] Agarwal A, Kumar S, Narang J, et al. Morphologic MRI features, diffusion tensor imaging and radiation dosimetric analysis to differentiate pseudo-progression from early tumor progression. J Neurooncol 2013;112:413—20.
[20] Akaike H. A Bayesian analysis of the minimum AIC procedure. In: Parzen E, Tanabe K, Kitagawa G, editors. Selected Papers of Hirotugu Akaike. New York: Springer; 1998. p. 275—80.
[21] Benjamini Y, Hochberg Y. Controlling the false discovery rate: a practical and powerful approach to multiple testing. J Royal Stat Soc 1995;57:289—300.
[22] Johnson DR, O'Neill BP. Glioblastoma survival in the United States before and during the temozolomide era. J Neurooncol 2012;107:359—64.
[23] Martino A, Krainik A, Pasteris C, et al. Neurological imaging of brain damages after radiotherapy and/or chimiotherapy. J Neuroradiol 2014;41:52—70.
[24] Bauchet L, Mathieu-Daude H, Fabbro-Peray P, et al. Oncological patterns of care and outcome for 952 patients with newly diagnosed glioblastoma in 2004. Neuro Oncol 2010;12:725—35.
[25] Shirai K, Suzuki Y, Okamoto M, et al. Influence of histological subtype on survival after combined therapy of surgery and radiation in WHO grade 3 glioma. J Radiat Res 2010;51:589—94.
[26] Robertson T, Koszyca B, Gonzales M. Overview and recent advances in neuropathology. Part 1: central nervous system tumours. Pathology 2011;43:88—92.
[27] Jain R, Poisson L, Narang J, et al. Genomic mapping and survival prediction in glioblastoma: molecular subclassification strengthened by hemodynamic imaging biomarkers. Radiology 2012;267:212—20.
[28] Moliterno JA, Patel TR, Piepmeier JM. Neurosurgical approach. Cancer J 2012;18:20—5.
[29] Kondo T. Mouse induced glioma-initiating cell models and therapeutic targets. Anticancer Agents Med Chem 2010;10:471—80.